ISSN 8755-6839

SCIENCE OF **TSUNAMI HAZARDS**

Journal of Tsunami Society International

Volume 39 **Number 4** **2020**

ESTIMATION OF RUPTURE DIRECTIVITY, CMT AND EARTHQUAKE TSUNAMI PARAMETERS AND THEIR CORRELATION WITH THE MAIN SOURCE OF THE FIRST TSUNAMI WAVE, SEPTEMBER 28, 2018

Madlazim[*],[1,2] Tjipto Prastowo,[1,2] and Muhammad Nurul Fahmi[3]

[1]*Physics Department, The State University of Surabaya, Surabaya 60231, INDONESIA. E-mail: madlazim@unesa.ac.id*

[2]*Center for Earth Science Studies, The State University of Surabaya, Surabaya 60231, INDONESIA*

[3]*Physics Department, Postgraduate Program, Institut Teknologi Sepuluh Nopember, Surabaya 60111, INDONESIA*

ABSTRACT

The purpose of this study is to analyze the main source of the Palu-Indonesia tsunami based on the direction of rupture, Centroid Moment Tensor (CMT), the tsunami parameters, including the rupture duration (T_{dur}), the 50 Seconds Exceed Duration (T50ex) and the dominant period (T_d) of the earthquake that occurred on September 28, 2018. The method employed in this study involves fitting the rupture duration versus seismic station azimuth graph to estimate the direction of the rupture, the full waveforms inversion method for determining the CMT and the direct procedure method for estimating tsunami parameters. The estimated direction of the earthquake rupture is azimuth 179°, which almost coincides with the Palu Koro Fault (PKF) azimuth. The direction of the earthquake rupture passed below the surface of the seawater in Palu Bay, which could possibly be the main source of the tsunami. The strike and dip of the nodal plane generated by the earthquake are 350° and 64°, respectively, which shows that a vertical displacement pushed seawater vertically in Palu Bay and caused the tsunami. All tsunami parameters from the earthquake exceeded the threshold; therefore, it is very likely that the earthquake was the main source of the first tsunami wave. The estimation results of the rupture directivity, Centroid Moment Tensor, and tsunami parameters are confirmed by inundation data that are qualitatively comparable with the observations.

Keywords: *Earthquake Rupture Duration; CMT; Tsunami Parameters; Tsunami Source; Inundation*

Vol 39 No. 4, page 228 (2020)

1. INTRODUCTION

A tectonic earthquake with a magnitude of 7.5 occurred some time ago around the Palu-Koro fault. The cause of the earthquake was speculated to be a submarine landslide, which could have caused tsunamis in Palu and Donggala on September 28, 2018. Even though three phenomena of earth disasters simultaneously occurred (earthquake, tsunami, and liquefaction), the most detrimental among the three phenomena was the tsunami phenomenon.

A tsunami is a phenomenon of sea surface wave propagation generated by the release of endogenous energy from the earth via the mechanism of tectonic earthquakes, submarine landslides, or other sources (Ward 2011). Large tsunamis associated with submarine strike-slip earthquakes are very rare. Strike-slip faults usually produce small tsunamis due to a lack of large vertical deformation (Gusman *et al.* 2017; Lay *et al.* 2018). However, the Palu-Koro fault zone that crosses Sulawesi Island is a strike-slip fault system in a complex tectonic region, which could facilitate vertical deformation. The strike-slip system may also include complicated fault geometry, such as nonvertical faults, arches, etc. This fault geometry can lead to complex fracture dynamics and produce a variety of pattern shifts during fractures, which can trigger tsunamis (Legg & Borrero 2001; Borrero *et al.* 2004).

Recorded history for local tsunamis generated by other strike-slip faults, such as the 1906 earthquake in San Francisco California, the 1994 earthquake in Mindoro Philippines, the 1999 earthquake in Izmit Turkey (Legg *et al.* 2003), and the 2016 Kaikoura earthquake in New Zealand (Power *et al.* 2017; Ulrich *et al.* 2019a). Large-scale strike-slip earthquakes can also produce tsunami aftershocks (Geist & Parsons 2005). We employ several ways to mitigate the tsunami disaster generated by the strike-slip fault system: first, by knowing the position and direction of the maximum main stress, intermediate stress and minimum stress from an area where strike-slip faults have been identified; second, by knowing the direction of the rupture caused by the September 28, 2018 earthquake; and third, a tsunami generated by the strike slip fault can also be analyzed using the tsunami parameters, namely, the rupture duration (T_{dur}), the duration greater than 50 seconds (T50ex) and the dominant period (T_d) (Lomax & Michelini 2011; Madlazim 2013).

Research on the direction of the rupture, which has been carried out by Madlazim (2011), provides results to estimate the direction of the rupture using short-period signals that have been recorded by two pairs of stations. If the duration of the rupture of the signal directed by the station is smaller than the signal recorded by the pairing station, then it can be interpreted that the direction of the rupture is toward this station. Madlazim *et al.* (2019) has also conducted research on the use of tsunami parameters for tsunami early warning applications 4 minutes after an earthquake. The results of the study indicated that a false warning was not issued for any of the 300 earthquakes that occurred in Indonesia. Tsunami parameters in the form of rupture duration (T_{dur}), duration greater than 50 seconds (T50ex) and dominant period (T_d) are useful to test whether the main source of the tsunami on September 28, 2018 is caused by seismic energy or landslides.

Tsunami parameters are useful for detecting whether an earthquake can cause a tsunami. Lomax & Michelini (2009b, 2011) have determined that the rupture length parameter of an earthquake is the most dominant parameter as an indicator of a tsunami, while it is

known that the rupture length is proportional to the earthquake rupture duration; so the earthquake rupture duration can be applied for early warning of tsunamis (Geist & Yoshioka 1996). In addition, the duration of the rupture can also provide additional information about the direction of the rupture, which can be useful for explaining how a tsunami could occur after the earthquake on September 28, 2018.

Centroid Moment Tensor (CMT) is the most complete and accurate information about earthquake sources; it has previously been investigated by many seismologists, including Kasmolan *et al.* (2010) and Ichinose *et al.* (2003). The Centroid Moment Tensor is utilized to determine the strike, dip and rake angles of an earthquake. Among these three angles, two angles are related to tsunami events, namely, the strike angle and the dip angle. The strike angle is determined from the North moving in a clockwise direction. Generally, the direction of the strike is the direction of the fault that caused the earthquake. The direction of earthquake rupture is usually in the direction of the fault that caused the earthquake. The dip angle illustrates the slope of the fault plane with respect to the horizontal plane. For a 90 ° dip angle, the fault plane is vertical. In this condition, it is not possible for an earthquake to generate a tsunami because there is no vertical displacement; so it is not possible to push vertical water above sea level.

The results of the calculation of the direction of the rupture, the Centroid Moment Tensor and tsunami parameters were confirmed with inundation data to determine the rational primary source of the tsunami on September 28, 2018, seismic energy or landslides. Researchers classified the research results related to the main source of tsunamis in Palu on September 28, 2018. There are 3 sources of tsunamis. First, the main source of tsunamis is seismic energy (Ulrich *et al.* 2019b). Second, the main source of tsunamis is landslide energy (Sepulveda *et al.* 2018; Heidarzadeh *et al.* 2019). Third, the main source of tsunamis is seismic energy, which is reinforced by landslide energy (Liu *et al.* 2018; van Dongeren *et al.* 2018).

In the research by Ulrich *et al.* (2019b), it has been concluded that the main source of the tsunami in Palu after the earthquake of September 28, 2018 was caused by seismic movements, which produced vertical movements that could cause tsunamis. This finding has been proven via earthquake dynamics modeling, in which the time and rupture speed, 3D geometric complexity of the fault, and effect of seismic waves on the propagation of the rupture are important parameters and is also supported by tsunami amplitude modeling and inundation height data.

In this study, we have discussed the main tsunami sources that were released from seismic earthquakes or landslides using analysis of the direction of rupture, Centroid Moment Tensor, and tsunami parameters that occurred after the Palu earthquake on September 28, 2018. Furthermore, the results of the estimation of the three seismic quantities were confirmed by the travel time data of the inundation recorded by the tide gauge around Palu Bay.

2. SETTING OF PALU-KORO FAULT

Sulawesi is located in the eastern part of Indonesia, which experiences high seismic activity. Sulawesi Island is located at the triple junction between the Sunda plate, Australian plate and Philippine Sea (Bellier *et al.* 2006; Socquet *et al.* 2006, 2019) (Fig. 1a). This condition can cause the area around Sulawesi to be very prone to earthquakes. The Australian Plate and Philippine Sea are

centered toward the Sunda plate due to the subduction and rotation zones of the Molucca Sea, Banda Sea and Timor Plate, which causes a complicated fault pattern.

The Central Sulawesi region is one of the earthquake prone areas in Indonesia because it is located near the source of earthquakes, which originates both on land and at sea. The source of an earthquake in the sea is the subduction of the Sulawesi and Molucca Sea Plates, while the source of an earthquake on land is several active faults on the mainland of Central Sulawesi, one of which was the Palu Koro Fault.

The Palu Koro fault, which is located along the Palu Koro valley and stretches from Palu Bay in the southeast direction, caused the Palu earthquake on September 28, 2018. This fault is the main geological structure in Central Sulawesi Province. According to the latest geodetic measurements, the Palu-Koro fault has a relatively high slip rate of 40 mm/year (Walpersdorf *et al.* 1998; Socquet *et al.* 2006), and according to geomorphology, the upper limit is 58 mm/year (Daryono 2018). The focal mechanism of the Palu-Koro fault indicated that it has a dip value of 65, which most likely caused the tsunami strike-slip earthquake that occurred on September 28, 2018 (Ulrich *et al.* 2019b). The Palu Koro fault has caused many tsunami disasters. According to Watkinson & Hall (2017), the Palu-Koro Fault is considered to pose a threat to the area through which it passes. Referring to previous data, four tsunamis were caused by the earthquake in the Palu-Koro fault that struck the northwest coast of Sulawesi in the past century (1927, 1938, 1968 and 1996) (Pelinovsky *et al.* 1997; Prasetya *et al.* 2001).

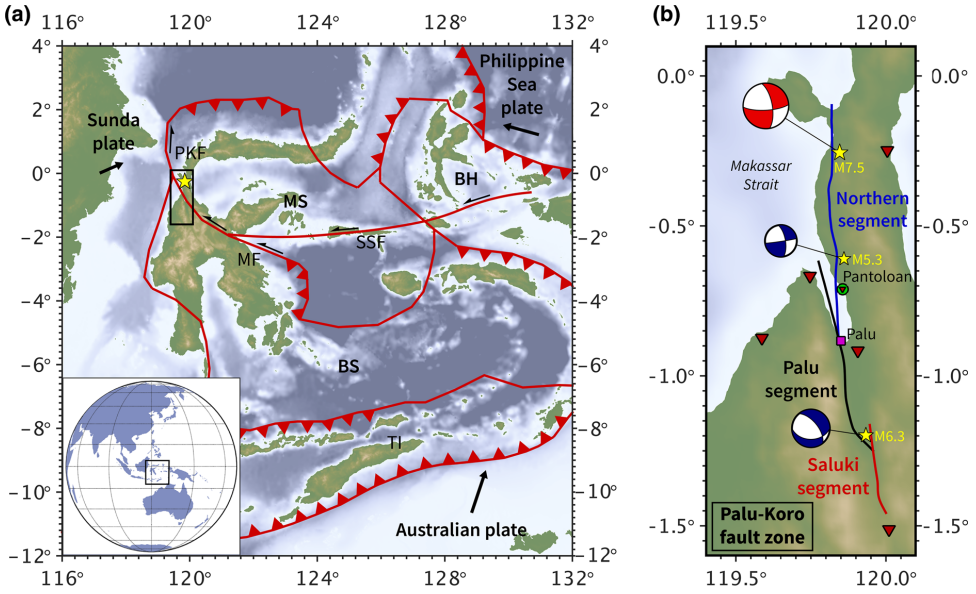

Fig. 1. (a) Tectonic structure of the Palu-Koro fault; the epicenter of the September 28, 2018 earthquake is marked by a yellow star (Ulrich et al., 2019b).

In Figure 1.(a) above the plate boundaries are marked with black lines that represent Bird (2003), Socquet *et al.* (2006), and Argus *et al.* (2011). PKF is the Palu-Koro fault zone; MF is the Matano fault zone; MS is the Molucca Sea plate; SSF is the Sula-Sorong fault zone; TI is the Timor plate; BH is the Bird's Head plate; and BS is the Banda Sea plate. The black arrows indicate the far-field plate velocities with respect to Eurasia (Socquet *et al.* 2006).

The black square represents the enlarged area at point (b), which is a magnification of the picture in the black box that shows the area where the earthquake occurred. The red triangle denotes an earthquake recording station. The focal mechanisms and epicenters of the earthquake on September 28, 2018 are shown: the top event was obtained from (USGS 2018), for the middle event is the aftershock earthquake on October 1, 2018 and the lowest event is the earthquake that occurred on January 23, 2005. The two latter events can be obstacles to the dip of the Palu-Koro fault.

3. METHODS

The method employed in this study is the method for fitting the data of rupture vs azimuth station seismic duration to estimate the direction of the rupture, the full waveforms inversion method for estimating earthquake CMT, and the direct procedure method for estimating tsunami parameters (rupture duration, dominant period, and 50 seconds exceed duration).

3.1. Estimation of Rupture Direction

The direction of the earthquake rupture can be estimated from the following equation. The duration of the rupture (T_{dur}) can be determined using the direct procedure for an earthquake seismogram, as expressed by Eq. (1).

$$Tdur = LVr - LVp\cos\theta \quad (1)$$

where L is the length of the rupture, Vr is the rupture speed, Vp is the phase velocity and θ is the angle between the azimuth station and the fault azimuth. The direction of the rupture can be estimated from Eq. (1) when the angle θ is zero, which means that T_{dur} has a minimum value (Hwang *et al.* 2011).

The duration of the rupture T_{dur} in Eq. (1) is estimated from the delay time after the arrival of the P wave for 90% ($T^{0,9}$), 80% ($T^{0,8}$), 50% ($T^{0,5}$), and 20% ($T^{0,2}$) from the peak value (Lomax & Michelini 2009a). The mathematical equation to calculate T_{dur} can be determined as follows:

$$Tdur = 1 - wT0,9 + wT0,2 \quad (2)$$

$$w = T0,2 + T0,52 - 2040s \quad (3)$$

with a limit of $T^{0,9} < T_{dur} < T^{0,2}$

T_{dur} can be estimated using seismogram data downloaded from the IRIS website, http://ds.iris.edu/wilber3/find_event. We employ the distance between the earthquake epicenter and the farthest seismic station, which is 40° from the azimuth station from 0° to 360°. Vertical component seismogram data from 56 seismic stations were utilized.

3.2. Full Waveform Inversion

The Centroid Moment Tensor from the September 28, 2018 earthquake can be determined by the full waveform inversion method developed by Ichinose *et al.* (2003). This method applies a three-component local waveform that is recorded by a seismic station and then estimated using the Green function. To calculate the Green function, we need a speed model for 1 dimension. The Green function is a picture of the signal to be recorded by a seismograph to obtain the model of the signal. The three-component Green function equation can be written as,

$$unx,t=Mij\xi,t*\partial \quad \partial\xi jGnjx,\xi,t\xi 0$$

$$Mij\xi,t*Gn,jx,\xi,t \qquad (4)$$

where un is the n-shift record, $Mij$is the 6 component moment tensor at the point of the earthquake source, ξ is the position of the earthquake source, x is the position of the receiver, Gn,j is a Green function depending on the elastic nature of the earth and the sign ($*$) shows convolution.

3.3. Estimation of Tsunami Parameters (T_{dur}, T_d, and T_{50ex})

To determine the values of the tsunami parameters, we employed the direct measurement procedure that has been developed by (Lomax & Michelini 2011; van Dongeren *et al.* 2018). The parameters for earthquakes can be determined via high frequency (HF) analysis of the vertical components of broadband seismograms that have been described in the study (Lomax *et al.* 2007; Lomax & Michelini 2009a, 2009b, 2011; Madlazim 2011), as shown in Eq. 5. T_d can be estimated using the direct method without inversion, which accelerates the process. To determine the dominant period (T_d), T_d is calculated using the time domain (τc) with the following equation (Nakamura 1988; Wu & Kanamori 2005; Lomax & Michelini 2013):

$$\tau c=2\pi T1T2v2tdtT1T2v2tdt \qquad (5)$$

where T_1 = 0 seconds (P onset) and T_2 = 55 seconds from a teleseismic earthquake seismogram (Lomax & Michelini 2009a). T_{50Ex} estimation was performed using the direct procedure of earthquake seismograms, namely, (1) filtering the velocity seismogram of vertical components using a high-frequency Butterworth filter (1-5 Hz), (2) automatically selecting P wave arrival times, (3) calculating the RMS amplitude (Ar) and the duration of 50 seconds after the arrival of P waves, (4) calculating T_{50Ex}, which is the ratio T50/Ar (Lomax & Michelini 2009b). Measurement of tsunami parameters caused by earthquakes in real time has been applied and can be accessed on the web http://aptsunami.fmipa.unesa.ac.id/www/

To estimate the tsunami parameters, T_{dur}, T_d, and T_{50Ex} in this study utilized seismogram data downloaded from the IRIS website: http://ds.iris.edu/wilber3/find_event. We apply the distance between the earthquake epicenter and the farthest seismic station at 15° with the azimuth of the station from 0° to 360°. Vertical component seismogram data recorded by 20 seismic stations were employed.

4. RESULTS AND DISCUSSION

The results of the estimated direction of the rupture, Centroid Moment Tensor (CMT) and tsunami parameters to test the main source of the tsunamis that occurred after the earthquake on September 28, 2018 are explained as follows:

4.1. Rupture Directivity

To estimate the direction of the earthquake rupture on September 28, 2018, we collected data from 56 seismic stations that have the closest azimuth, whose value is 1.82° to the station that has the furthest azimuth value of 356,83°. We calculated the value of rupture duration (T_{dur}) for each station.

The blue dots in Fig. 2 represent the earthquake rupture duration data for each azimuth; they are fitted to form a red line. On the red line, two hills of waves and 1 valley of waves are formed, which means that on the two hills of waves, a high average T_{dur} value occurs at azimuth 1.82° to 6.89° and 255.84° to 356.83°, whereas a low average T_{dur} value occurs at azimuth 140.33° to 193.28°, for 1 valley. In the data, we the lowest T_{dur} value of 10.8 s occurred on the 179° azimuth. To determine the direction of the rupture, the smallest T_{dur} value is interpreted as the direction of the rupture, according to the results of the study by Hwang *et al.* (2011) and Madlazim (2011). If the duration of the rupture of the signal recorded by the station is smaller than the signal recorded by the other station, then it can be interpreted that the direction of the rupture is oriented toward this station.

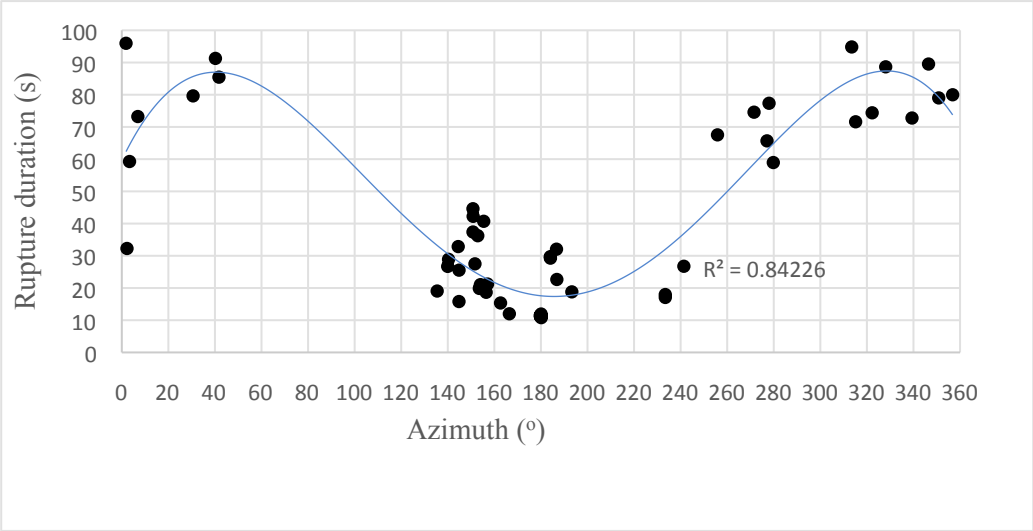

Fig. 2. Relationship between the duration of rupture (T_{dur}) with the azimuth seismic station that records data waveforms. In this graphic, there are 56 data points from the station that recorded the earthquake on September 28, 2018.

In the case of September 28, 2018, the direction of the rupture moved in the direction of the azimuth 179°, which means that it almost coincides with the Palu-Koro Fault zone (Fig. 1b). Thus, the direction of the rupture passes through the underwater segment of the Palu bay, where according to research by Heidarzadeh *et al.* (2019), the maximum tsunami wave heights at two tidal gauge stations, Pantoloan (in Palu Bay) and Mamuju (outside Palu Bay) are 380 cm and 24 cm, respectively. This finding is correlated with Ulrich *et al.* (2019b), who concluded that the tsunami that occurred after the September 28, 2018 earthquake was largely localized in Palu Bay. Thus, the estimation results of this rupture direction are consistent with the results of the study, which indicates the main source of the tsunami that occurred after the September 28, 2018 earthquake was a seismic earthquake. The results of this study are supported by the results of research by Ulrich *et al.* (2019b) and Madlazim *et al.* (2019).

4.2. Centroid Moment Tensor

Part of the results of the CMT estimation are strike, dip, and rake values in the September 28, 2018 earthquake. Fig. 3 shows the results of a description of the full waveform fitting between observed data and synthetic data that have been calculated by the Green function. Each seismic station that records an earthquake has three local components that are observed and symbolized as T for the tangential component, R for the radial component, and Z for the vertical component. Black waveforms indicate waveforms obtained from observational data, while red waveforms indicate synthetic waveforms obtained from calculations. The matching level of local fitting full waveforms between synthetic signals (red) and observed signals (black) is expressed by the percentage value of Variance Reduction (VR). The full-waveform inversion in this study employs a frequency of 0.02 Hz to 0.05 Hz and uses a 3-component local signal recorded by 5 seismic stations (Fig. 4), which causes a Variance Reduction (VR) value of 81%. If the VR value exceeds 50%, the results of the CMT solution can be categorized as reliable (Vackář *et al.* 2017).

The value of the focal mechanism at the source modeled in this study are strike, dip, and rake angles of 350°, 64°, and -6°, respectively, which is very close to the value of the focal mechanism released by USGS, namely, 350°, 65°, and -17°. The 350 ° strike angle corresponds to the Palu-Koro Fault (PKF) direction. From this strike angle, it can be seen that the direction of the rupture that leads to the station passed through Palu bay. The dip angle of 64 ° is almost the same as the CMT estimate of Ulrich *et al.* (2019b). The dip angle of 64 ° indicates a shift in the vertical component, which pushed seawater vertically and caused the tsunami. The same results were also obtained by Ulrich *et al.* (2019b), who discovered that the dip value from the Palu-Indonesia earthquake on September 28, 2018, is 65°. Fig. 4 is an image of the station distribution map utilized in this study. We employed 5 stations (SMKI.IA SGKI.IA BKB.IA, TOLI2.IA, and LUWI.IA), whose positions include the earthquake epicenter and earthquake focal mechanism (Fig. 4).

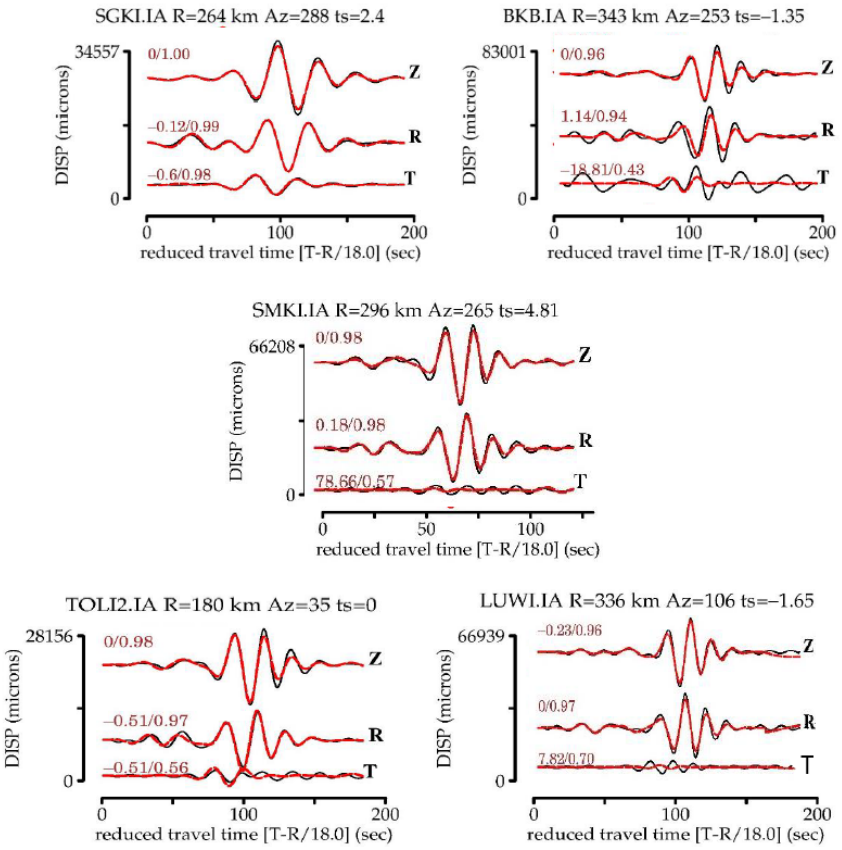

Fig. 3. Results of full waveform inversions between synthetic data and earthquake observation data on September 28, 2018.

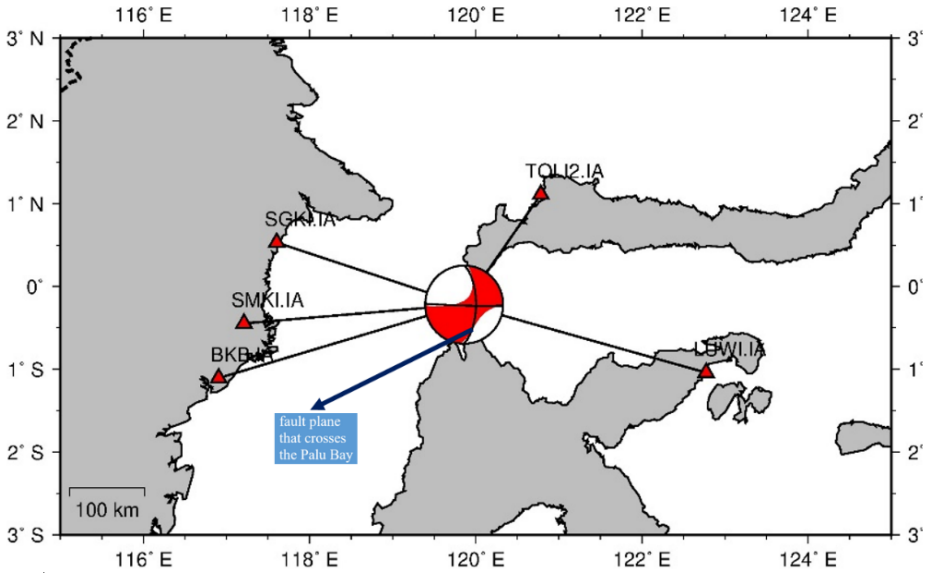

Fig. 4. Results distribution map of 5 seismic stations and earthquake beach ball on September 28, 2018, whose direction of strike angle passes through Palu Bay, which corresponds to the direction of the PKF (Ulrich *et al.* 2019b).

4.3. Tsunami Parameters

Three tsunami parameters are applied to indicate whether an earthquake has the potential to cause a tsunami. The three tsunami parameters are the duration of rupture (T_{dur}), dominant period (T_d) and 50 Seconds Exceed Duration (T_{50Ex}). If the T_{dur} exceeds or is equal to the 65-second threshold, an earthquake has the potential to cause a tsunami. If the T_{dur} is less than the threshold, the earthquake has no tsunami potential. If T_d exceeds or is equal to the 10-second threshold, an earthquake has the potential to cause a tsunami. If T_d is less than the threshold, then an earthquake has no tsunami potential. If T_{50Ex} exceeds or equals a threshold of 1, an earthquake has the potential to cause a tsunami. If T_{50Ex} is less than the threshold, then an earthquake has no tsunami potential. The following examples present the results of the T_{dur}, T_d and T_{50Ex} estimates from the earthquake seismogram on September 28, 2018, as recorded by the PLAI seismic station, where all three tsunami parameters exceed the threshold.

Data from the estimated tsunami parameters from an average of 20 seismic stations employed in this study are presented in Table 1 as follows:

All tsunami parameters estimation results presented in Table 1 exceed the threshold. Thus, the results of the estimated tsunami parameters support the hypothesis that the main source of the tsunamis that occurred after the September 28, 2018 earthquake was a seismic earthquake. The results of this study are supported by the results of research by Ulrich *et al.* (2019b) and Madlazim *et al.* (2019).

Simulations of inundation heights at various locations around Palu Bay, where observations have been recorded by Ulrich *et al.* (2019b) and then observed with some estimates, yielded inundation data that was too high in the northern boundary of Palu bay and a little too low in the southern part near the Grandmall of Palu City. These findings conclude that large errors at the height of the inundation are randomly distributed and the inundation originates from the effect of local amplification, which cannot be captured in the scenario due to a lack of bathymetry/topographic resolution. The maximum water depth is calculated from the tsunami scenario near Palu City. Qualitatively, the results of this scenario are quite consistent with the observations, because the depth of the largest puddle is close to the Grandmall area, where major damage from the tsunami was reported. Tsunami scenarios stem from seismic displacement from dynamics. Earthquake rupture scenarios produce inundations that are qualitatively comparable to available observations. The wave amplitude and the height of the puddle fits well given the limited quality of available topographic data (Ulrich *et al.* 2019b).

All tsunami parameters from the earthquake on September 28, 2018 exceed the threshold; so it is very likely that earthquakes are the main source of tsunamis. The estimated results of the rupture direction, CMT, and tsunami parameters are confirmed by waterlogging data that are qualitatively comparable with available observations. The wave amplitude matches well (Ulrich *et al.* 2019b).

Table 1. Average values of the tsunami parameters for the September 28, 2018 earthquake

T_{dur} (s)	T50Ex	T_d (s)	$T_{dur}*T_d$ (s^2)	T_d*T50Ex (s)
93.01	2,01	10.39	966.47	21.50

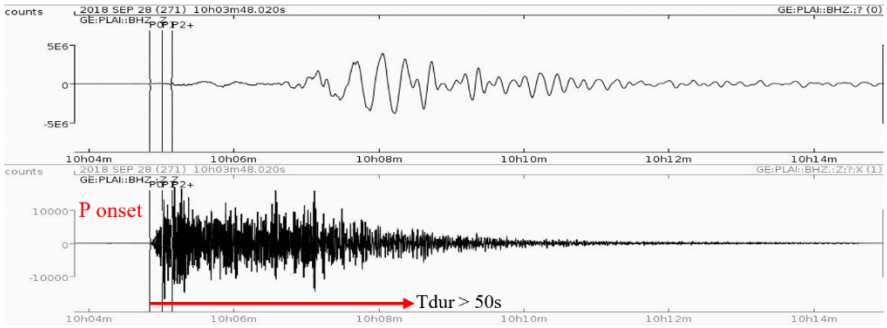

Fig. 5. Seismogram recorded by PLAI station (above), Rupture Duration (T_{dur}) = 120.0s.

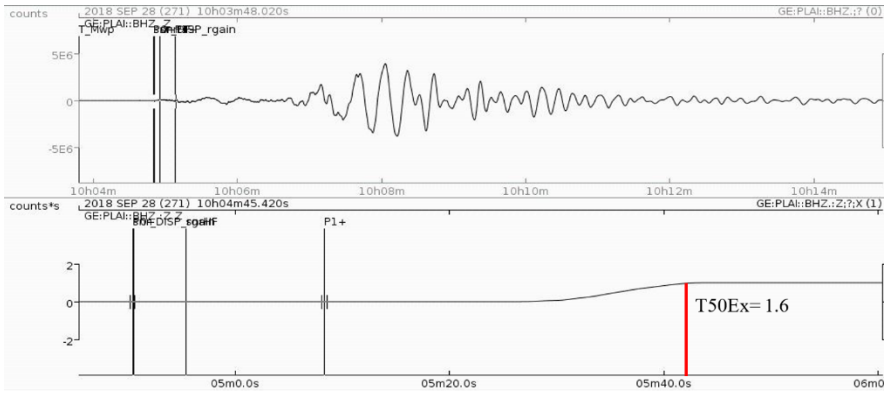

Fig. 6. Seismogram recorded by PLAI station (above), Exceed duration (T_{50Ex}) = 1.6.

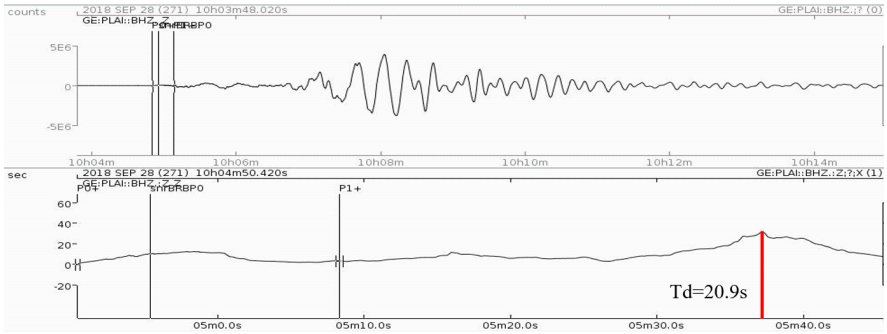

Fig. 7. Seismogram recorded by PLAI station (above), dominant period (T_d) = 20.9 s.

Based on the observations as shown in the video which can be accessed at the following link https://www.youtube.com/watch?v=y0UOfVr7jBE . There were three tsunami waves after the Palu earthquake on September 28, 2018. The height of the first tsunami wave was not too big, on average, it was around 0.8 meters, but it was enough to make the people around the Palu Strait coast surprised because previously the tsunami early warning had been canceled. This

first tsunami wave was generated by the seismic energy from the earthquake. Meanwhile, the height of the second and third tsunami waves on the coast of the Palu Strait was very large, more than 6 meters. This could not have been caused by a strike-slip type earthquake, but it is very likely that it was caused by a landslide whose water waves were amplifying.

5. CONCLUSIONS

Based on the estimation of the direction of the rupture, the rupture moves in the direction of the azimuth 179°, which means that it passes under Palu bay, where there is a maximum tsunami wave height. The results of the CMT solution are in the form of a strike angle of 350°, which corresponds to the PKF direction and rupture direction. A dip angle of 64° indicates the existence of a vertical displacement component that can push the water in Palu bay, which eventually causes a tsunami. The tsunami parameter estimation results also support that the main source of tsunamis that occurred after the earthquake on September 28, 2018, was a seismic earthquake because all tsunami parameters exceed the threshold. Thus, it is very likely that earthquakes comprise the main source of the first tsunamis wave. The estimation results of the direction of the rupture, CMT, and tsunami parameters are confirmed by inundation data from tsunamis, bathymetry/topography, in which there is a wave height of seawater.

ACKNOWLEDGMENTS

The authors sincerely thank the Indonesian Agency for Geophysics, Climatology, and Meteorology (BMKG) Indonesia for providing the earthquake data employed in this study, GEOFON GFZ and Incorporated Research Institutions for Seismology (IRIS) for the seismic data were available from their respective sites at http://eida.gfz-potsdam.de/webdc3/ and http://www.iris.edu/wilber3/find. This article has also benefited from constructive reviews from two anonymous reviewers. We also thank the Ministry of Education and Culture's DRPM for supporting this research. This work is funded by DRPM, The Ministry of Education and Culture, The Republic of Indonesia under grant number B/11632/UN38.9/LK.04.00/2020.

REFERENCES

Argus, D.F., Gordon, R.G. & DeMets, C., 2011. Geologically current motion of 56 plates relative to the no-net-rotation reference frame, *Geochem. Geophys. Geosystems*, 12, Q11001.

Bellier, O., Sébrier, M., Seward, D., Beaudouin, T., Villeneuve, M. & Putranto, E., 2006. Fission track and fault kinematics analyses for new insight into the Late Cenozoic tectonic regime changes in West-Central Sulawesi (Indonesia), *Tectonophysics*, 413, 201–220.

Bird, P., 2003. An updated digital model of plate boundaries, *Geochem. Geophys. Geosystems*, 4, 1027.

Borrero, J.C., Legg, M.R. & Synolakis, C.E., 2004. Tsunami sources in the Southern California bight, *Geophys. Res. Lett.*, 31, 211.

Daryono, M.R., 2018. Paleoseismologi tropis Indonesia (dengan studi kasus di Sesar Sumatra, Sesar Palukoro-Matano, Dan Sesar Lembang). Available at: http://docplayer.info/111161004-Paleoseismologi-tropis-indonesia-dengan-studi-kasus-di-sesarsumatra-sesar-palukoro-matano-dan-sesar-lembang-disertasi.html, Accessed September 2019.

Geist, E. & Yoshioka, S., 1996. Source parameters controlling the generation and propagation of potential local tsunamis along the Cascadia margin, *Nat. Hazards*, 13, 151–177.

Geist, E.L. & Parsons, T., 2005. Triggering of tsunamigenic aftershocks from large strike-slip earthquakes: analysis of the November 2000 New Ireland earthquake sequence, *Geochem. Geophys. Geosystems*, 6, Q10005.

Gusman, A.R., Satake, K. & Harada, T., 2017. Rupture process of the 2016 Wharton Basin strike-slip faulting earthquake estimated from joint inversion of teleseismic and tsunami waveforms, *Geophys. Res. Lett.*, 44, 4082–4089.

Heidarzadeh, M., Muhari, A. & Wijanarto, A.B., 2019. Insights on the source of the 28 September 2018 Sulawesi Tsunami, Indonesia based on spectral analyses and numerical simulations, *Pure Appl. Geophys.*, 176, 25–43.

Hwang, R.-D., Chang, J.-P., Wang, C.-Y., Wu, J.-J., Kuo, C.-H., Tsai, Y.-W., Chang, W.-Y. & Lin, T.-W., 2011. Rise time and source duration of the 2008 MW 7.9 Wenchuan (China) earthquake as revealed by Rayleigh waves, *Earth Planets Space*, 63, 427–434.

Ichinose, G., Anderson, J., Smith, K. & Zeng, Y., 2003. Source parameters of Eastern California and Western Nevada earthquakes from regional moment tensor inversion, *Bull. Seismol. Soc. Am.*, 93, 61–84.

Kasmolan, M., Santosa, B.J., Lees, J.M. & Utama, W., 2010. Earthquake source parameters at the sumatran fault zone: identification of the activated fault plane, *Cent. Eur. J. Geosci.*, 2, 455–474.

Lay, T., Ye, L., Bai, Y., Cheung, K.F. & Kanamori, H., 2018. The 2018 MW 7.9 Gulf of Alaska earthquake: multiple fault rupture in the Pacific plate, *Geophys. Res. Lett.*, 45, 9542–9551.

Legg, M.R. & Borrero, J.C., 2001. Tsunami potential of major restraining bends along submarine strike-slip faults, in *Proceedings of the International Tsunami Symposium*, pp. 331–342, NOAA/PMEL.

Legg, M.R., Borrero, J.C. & Synolakis, C.E., 2003. Tsunami hazards from strike-slip earthquakes. American Geophysical Union, Fall Meeting 2003, abstract id OS21D-06. Available at: http://docplayer.info/111161004-Paleoseismologi-tropis-indonesia-dengan-studi-kasus-di-sesarsumatra-sesar-palukoro-matano-dan-sesar-lembang-disertasi.html, Accessed September 2019.

Liu, P.L.F., Barranco, I., Fritz, H.M., Haase, J.S., Prasetya, G.S., Qiu, Q., Sepulveda, I., Synolakis, C. & Xu, X., 2018. What we do and don't know about the 2018 Palu Tsunami—a future plan. In AGU fall meeting 2018. Available at: https:// agu.confex.com/agu/fm18/meetingapp.cgi/Paper/476669, Accessed 2019.

Lomax, A. & Michelini, A., 2009a. Mwpd: a duration–amplitude procedure for rapid determination of earthquake magnitude and tsunamigenic potential from P waveforms, *Geophys. J. Int.*, 176, 200–214.

Lomax, A. & Michelini, A., 2009b. Tsunami early warning using earthquake rupture duration, *Geophys. Res. Lett.*, 36, L09306.
Lomax, A. & Michelini, A., 2011. Tsunami early warning using earthquake rupture duration and P-wave dominant period: the importance of length and depth of faulting, *Geophys. J. Int.*, 185, 283–291.
Lomax, A. & Michelini, A., 2013. Tsunami early warning within five minutes, *Pure Appl. Geophys.*, 170, 1385–1395.
Lomax, A., Michelini, A. & Piatanesi, A., 2007. An energy-duration procedure for rapid determination of earthquake magnitude and tsunamigenic potential, *Geophys. J. Int.*, 170, 1195–1209.
Madlazim, 2011. Toward Indonesian tsunami early warning system by using rapid rupture durations calculation, *Sci. Tsunami Hazards*, 30, 233–243.
Madlazim, 2013. Assessment of tsunami generation potential through rapid analysis of seismic parameters-case study: comparison of the sumatra earthquakes of 6 April and 25 October 2010, *Sci. Tsunami Hazards*, 32, 29–38.
Madlazim, Rohadi, S., Koesoema, S. & Meilianda, E., 2019. Development of tsunami early warning application four minutes after an earthquake., *Sci. Tsunami Hazards*, 38, 132–141.
Nakamura, Y., 1988. On the urgent earthquake detection and alarm system (UrEDAS), in *Proceedings of the 9th World Conference on Earthquake Engineering,* pp. 673–678, Tokyo-Kyoto.
Pelinovsky, E., Yuliadi, D., Prasetya, G. & Hidayat, R., 1997. The 1996 Sulawesi tsunami, *Nat. Hazards*, 16, 29–38.
Power, W., Clark, K., King, D.N., Borrero, J., Howarth, J., Lane, E.M., Goring, D., Goff, J., Chagué-Goff, C., Williams, J., Reid, C., Whittaker, C., Mueller, C., Williams, S., Hughes, M.W., Hoyle, J., Bind, J., Strong, D., Litchfield, N. & Benson, A., 2017. Tsunami runup and tide-gauge observations from the 14 November 2016 M7.8 Kaikōura earthquake, New Zealand, *Pure Appl. Geophys.*, 174, 2457–2473.
Prasetya, G.S., De Lange, W.P. & Healy, T.R., 2001. The makassar strait tsunamigenic region, Indonesia, *Nat. Hazards*, 24, 295–307.
Sepulveda, I., Haase, J.S., Liu, P.L.F., Xu, X. & Carvajal, M., 2018. On the contribution of co-seismic displacements to the 2018 Palu tsunami. In AGU Fall Meeting 2018. Available at: https://agu.confex.com/agu/fm18/meetingapp.cgi/Paper/476669, Accessed September 2019.
Socquet, A., Hollingsworth, J., Pathier, E. & Bouchon, M., 2019. Evidence of supershear during the 2018 magnitude 7.5 Palu earthquake from space geodesy, *Nat. Geosci.*, 12, 192–199.
Socquet, A., Simons, W., Vigny, C., McCaffrey, R., Subarya, C., Sarsito, D., Ambrosius, B. & Spakman, W., 2006. Microblock rotations and fault coupling in SE Asia triple junction (Sulawesi, Indonesia) from GPS and earthquake slip vector data, *J. Geophys. Res. Solid Earth*, 111, B08409.
Ulrich, T., Gabriel, A.-A., Ampuero, J.-P. & Xu, W., 2019a. Dynamic viability of the 2016 Mw 7.8 Kaikōura earthquake cascade on weak crustal faults, *Nat. Commun.*, 10, 1213.

Ulrich, T., Vater, S., Madden, E.H., Behrens, J., van Dinther, Y., van Zelst, I., Fielding, E.J., Liang, C. & Gabriel, A.A., 2019b. Coupled, physics-based modeling reveals earthquake displacements are critical to the 2018 Palu, sulawesi tsunami, *Pure Appl. Geophys.*, 176, 4069–4109.

USGS, 2018. Available at: https://earthquake.usgs.gov/earthquakes/eventpage/us1000h3p4/moment-tensor, Accessed September 2019.

Vackář, J., Burjánek, J., Gallovič, F., Zahradník, J. & Clinton, J., 2017. Bayesian ISOLA: new tool for automated centroid moment tensor inversion, *Geophys. J. Int.*, 210, 693–705.

van Dongeren, A., Vatvani, D. & van Ormondt, M., 2018. Simulation of 2018 tsunami along the coastal areas in the palu bay. In AGU fall meeting 2018. Available at: https://agu.confex.com/agu/fm18/meetingapp.cgi/Session/66627, Accessed September 2019.

Walpersdorf, A., Rangin, C. & Vigny, C., 1998. GPS compared to long-term geologic motion of the North arm of Sulawesi, *Earth Planet. Sci. Lett.*, 159, 47–55.

Ward, S.N., 2011. Encyclopedia of solid earth geophysics: tsunami, in *National Geophysical Research Institute (NGRI). Council of Scientific and Industrial Research (CSIR)*, pp. 1–1539, ed. Gupta, H. K. Springer Netherlands.

Watkinson, I.M. & Hall, R., 2017. Fault systems of the Eastern Indonesian triple junction: evaluation of quaternary activity and implications for seismic hazards, *Geol. Soc. Lond. Spec. Publ.*, 441, 71.

Wu, Y. & Kanamori, H., 2005. Experiment on an onsite early warning method for the taiwan early warning system, *Bull. Seismol. Soc. Am.*, 95, 347–353.